GRAVITATIONAL WAVES FROM NEUTRON STARS: DETECTION PROSPECTS AND INFERENCES FOR TWO DISTINCT TYPES OF REMNANTS*

José A. Font

Departamento de Astronomía y Astrofísica, Universitat de València
Dr. Moliner 50, 46100, Burjassot (València), Spain
and
Observatori Astronòmic, Universitat de València
Catedrático José Beltrán 2, 46980, Paterna (València), Spain

Received 4 March 2025, accepted 4 March 2025,
published online 22 April 2025

The detection of gravitational waves from compact binary coalescences is impacting our knowledge of stellar-origin compact objects. In particular, gravitational waves from neutron stars encode key information about the nature of matter at nuclear densities and above. Its gravitational-wave spectrum is linked to neutron star properties and can be used to impose constraints on the equation of state, complementing those obtained by electromagnetic observations or heavy-ion experiments. In turn, those constraints can be used to infer key properties as the masses and radii of neutron stars, their tidal deformability, or their moment of inertia. Numerical simulations of neutron stars, either in compact binary systems or those formed in supernova explosions, are fundamental to assist in the detection of the gravitational waves they emit. Simulations are also essential for understanding their formation in highly dynamical events and assessing the role they play across various fields: relativistic astrophysics (as the central engine of gamma-ray bursts and kilonovae), gravitational physics (as prime sources of gravitational waves), cosmology (as standard sirens), and nuclear physics (to constrain the equation of state). In this article, we review the prospects to detect gravitational waves from two "types" of neutron stars — the hypermassive neutron star resulting from the merger of two neutron stars in a binary system, and the proto-neutron star born after the gravitational collapse of the core of a sufficiently massive progenitor star. Moreover, we also discuss ongoing efforts to infer parameters of the source from the analysis of the gravitational-wave signals and the wealth of physical information that can potentially be extracted.

DOI:10.5506/APhysPolB.56.5-A1

* Presented at the LXIV Cracow School of Theoretical Physics *From the UltraViolet to the InfraRed: a panorama of modern gravitational physics*, Zakopane, Poland, 15–23 June, 2024.

1. Introduction

After the momentous observation of GW150914, the first gravitational-wave (GW) signal ever detected [1], GW science is rapidly becoming an exciting field of research. GW150914 originated in the coalescence and merger of two stellar-origin black holes in a compact binary system. Since then, the LIGO–Virgo–KAGRA (LVK) Collaboration, which operates the network of ground-based detectors Advanced LIGO [2], Advanced Virgo [3], and KAGRA [4], have reported nearly one hundred compact binary coalescence (CBC) events during their first three observing runs [5, 6]. Those observations include all three classes of CBC systems, namely, binary black holes (BBH), binary neutron stars (BNS), and black-hole–neutron star (BHNS) systems. The latter two are prime targets for multi-messenger observations, being visible in both GW, electromagnetic (EM) radiation, and possibly also accessible to neutrino telescopes. Catalogues of BBH mergers in primary masses 5–60 $M_\odot$ have been assembled, allowing to place constraints on astrophysical populations of sources and on cosmological parameters [7–9]. Moreover, the detection of the GW signal from the first BNS merger, along with its post-merger EM emission, GW170817 [10–13], is helping address some long-standing issues in relativistic astrophysics such as the association between BNS mergers, short gamma-ray bursts, and their optical afterglows (*i.e.* the kilonovae, powered by the radioactive decay of heavy r-process nuclei), the nature of the equation of state (EoS) of matter at supranuclear densities, the radius and tidal deformability of neutron stars, the speed of GW (ruling out, in turn, a large class of scalar–tensor theories), and has even allowed for independent measures of the Hubble constant.

The physics program of the LVK Collaboration involves the study of transient GW signals such as CBC events and bursts (*e.g.* supernovae), longer signals (*e.g.* the nearly monochromatic continuous signals produced by spinning neutron stars), and stochastic GW backgrounds. The latter are a consequence of the superposition of the GW produced by a large number of unresolved, independent sources, such as BBH and BNS mergers, but also from other types of sources both transient, as supernovae or mergers of white dwarf binaries, and continuous, as spinning neutron stars or magnetars (see [14] and references therein).

All events detected so far by the LVK Collaboration are consistent with CBC events. An important aid to the detection of these sources is the fact that their inspiral can be accurately modelled using combinations of analytic relativity and numerical relativity techniques. To dig CBC signals out of the detector noise, CBC searches are based on matched-filtering using banks of waveform templates from general relativity. Huge amounts of templates are required to assist both in detection and parameter estimation. Unfortunately, banks remain incomplete in some regions of the parameter space of CBC sources, *e.g.* for large component mass ratios, for misaligned spins (*i.e.* different orientations between the individual spins and the orbital angular momentum vector) yielding to precessing orbits, or for non-quasi-circular, eccentric, orbits. Numerical relativity — the numerical solution of Einstein's field equations coupled to hydrodynamics for the two-body problem — is our best tool to model CBC waveforms. However, not only the physics current simulation codes incorporating is to some extent still incomplete (particularly for non-vacuum systems) but also the simulations themselves are intrinsically very expensive from a computational viewpoint. To ameliorate this, the synergy between numerical relativity and analytical relativity has become fundamental to extract all transient GW signals reported by the LVK Collaboration (see [15] and references therein). In addition, there is great hope that approaches based on Machine Learning and AI may help complete CBC template banks, aiding both searches and parameter estimation. Aspects still to be improved are diverse, including the increase in the component mass ratio and harmonic content, accounting for non-quasi-circular orbits (eccentricity, dynamical captures, hyperbolic encounters), decreasing systematic errors, or even building waveform models for mergers of exotic compact objects or in gravity theories beyond general relativity.

CBC sources are the prime sources for GW astronomy and the loudest systems for the LVK detector network. Among the yet undetected sources, Core-Collapse Supernovae (CCSN) emit GW at frequencies that make them perfect targets for ground-based detectors. The progenitors of CCSN are typically non-rotating stars with masses in the range of 8–100 $M_\odot$ [16, 17]. Despite the fact that a CCSN is a very energetic event, with a binding energy of about $E_{\rm bin} \sim 10^{53}$ erg, the deformation of spacetime it produces and the associated GW amplitude is fairly small, $E_{\rm GW} < 10^{-6} E_{\rm bin}$. Since the strength of a typical CCSN GW signal is significantly smaller than that of CBC sources, realistic detectability prospects of CCSN events are limited to distances within 10 kpc, *i.e.* Galactic events, for current detectors [18, 19]. This strongly impacts the chances of detection as CCSN events are rare, with rates of about one event every 30 years in our Galaxy [20]. In addition, GW signals from CCSN are quite complex and, contrary to CBC systems, they cannot be easily modelled as the post-bounce signal has a distinctive stochastic nature (dominated by convective turbulence). For this reason, numerical simulations of CCSN are highly necessary.

Despite the difficulties, a successful detection of a CCSN GW signal would be a scientifically highly rewarding event as it could potentially reveal the underlying explosion mechanism through the analysis of the waveform along with physical properties of the progenitor star and of the remnant, the new-born proto-neutron star (PNS). Hours after the collapse of the massive star's core, the supernova shock breaks through the stellar surface. The supernova explosion is then seen as an EM phenomenon. The light curve yields indirect information about the core collapse mechanism as it is an "echo" of the supernova driving engine. In order to look at the "heart" of a supernova, we can use two messengers complementary to light, namely neutrinos and GWs. Neutrinos stream out seconds after the collapse. Their flux decays with the square of the distance, challenging its detection and most likely limiting it to Galactic CCSN events. Correspondingly, GWs decouple from matter directly after they are generated and are hence fully synchronised with the core collapse. Compared to the flux of neutrinos, the amplitude of the GW signal decays linearly with distance, which might help detecting an extragalactic CCSN event in the future, once third-generation GW observatories Einstein Telescope and Cosmic Explorer become operational [21, 22].

GW searches from CCSN are an essential activity in the LVK Collaboration physics program. Unlike CBC searches, in the case of CCSN (and other types of burst signals), the searches are not based on matched filtering, as CCSN are unmodelled GW sources. The typical ingredients of an unmodelled search pipeline comprise the cross-correlation of the data collected in pairs of detectors and the analysis of possible excess power, usually through coherent combinations of data from several GW detectors. This allows to look for signals in the sensitive band (from about 20 Hz to 2 kHz) with duration from about 1 ms to 1 s. Some of the most widely used LVK CCSN search pipelines are coherent Wave Burst [23], X-pipeline [24], and BayesWave [25].

First CCSN searches were initiated in 2016 with the Initial LIGO and Initial Virgo detectors (and GEO600) [26]. In this study, GW data coincident with 2 CCSN observed optically in 2007 and 2011 (within 15 Mpc) was analysed. Three families of artificial GW waveforms were injected into the data: stochastic waveforms from 2D and 3D numerical simulations of CCSN events, waveforms from semi-analytical calculations for models of extreme emission of known shape (bar-mode deformation and torus fragmentation instability), and phenomenological sine-Gaussian waveforms. The latter probe specific combinations of signal frequency and time intervals, and allow to compute upper limits on the GW energy. The study conducted in [26] reported no GW but allowed to place upper limits on the amount of GW energy that could have been emitted by the two supernovae considered ($\sim 0.1Mc^2$ at low frequencies to $\sim 10Mc^2$ at frequencies above 1 kHz). This initial search could not constrain or exclude any of the CCSN models considered.

The most recent CCSN search conducted by the LVK Collaboration has used data from O3, the third observing campaign of the detector network [27]. This study searched for GW transients associated with 8 CCSN observed optically within 30 Mpc during O3. As in previous cases, no GW association was identified (which was not unexpected due to the distance range of the sources considered). The study allowed to analyse the detection efficiency for a variety of possible GW emission mechanisms in CCSN, namely neutrino-driven and magneto-rotational explosions, black hole formation, QCD phase transitions, and extreme models of collapse leading to the formation of long-lasting bars in the PNS. The results reported in [27] placed more stringent upper limits on the distance reach of CCSN searches, on the GW energy and luminosity, and on the PNS ellipticity.

In the remainder of this paper, we will discuss the GW modelling of neutron stars both in BNS mergers and in CCSN, providing an overview of selected recent results. For the case of BNS mergers, we will highlight the importance of finite-temperature effects in the long-term dynamics of the remnant and on the GW emission, the detectability prospects of high-frequency features present in the late-time spectrum, and the role non-convex EoS may play in the merger dynamics and how their effects might challenge the interpretation of physical results. Correspondingly, for the CCSN system, we will discuss how the analysis of the waveforms associated with the oscillation modes of the PNS may help design a detection strategy and will discuss inference prospects in the particular case of rotational CCSN progenitors.

2. GW modelling of neutron stars in BNS mergers and CCSN

2.1. BNS mergers

Modern waveform models of BNS merger signals produce a complete waveform through its inspiral stage up to merger by relying either on semi-analytical procedures, typically using effective-one-body (EOB) and phenomenological modelling, or a fully data-driven approach as in so-called surrogate models [28]. In particular, prior to merger, the signal is well described using approximations from analytical relativity by performing an iterative procedure to obtain corrections to the Newtonian dynamics (post-Newtonian expansion), and corrections to flat spacetime accounting for the GW emission (post-Minkowskian expansion). There is a large body of work on these approaches, in particular for quasi-circular binaries in the adiabatic approximation (see [29] for a review). Post-Newtonian waveform approximants currently include high-order tidal corrections, dynamical tidal effects, and spin-tidal couplings. On the other hand, the EOB approach [30–32] describes the two-body dynamics in general relativity and its GW emission employing a resummation of the post-Newtonian information for the dynamics in terms of the geodesic motion of a particle in an effective spacetime. Present-day tidal waveform models for BNS mergers are mostly based on the EOB approach.

As illustrated in Fig. 1, the computation of the BNS post-merger waveform (not plotted on purpose) is the current frontier. Its analytic modelling is not possible and numerical relativity is the only reliable tool to produce waveforms. This part of the signal strongly depends on the many physical ingredients that need to be included in the modelling. Contrary to vacuum systems such as BBH mergers, a faithful numerical description of BNS mergers must not only solve Einstein's field equations but also the magneto-hydrodynamics equations for the matter fields, capture the amplification of the magnetic field during merger and post-merger (as a result of the Kelvin–Helmhotz and magneto-rotational instabilities), and handle the nuclear matter EoS, non-ideal viscous effects, or the transport of neutrinos. Each of those ingredients impacts the fate of the remnant in a significant way and, hence, the associated gravitational waveforms.

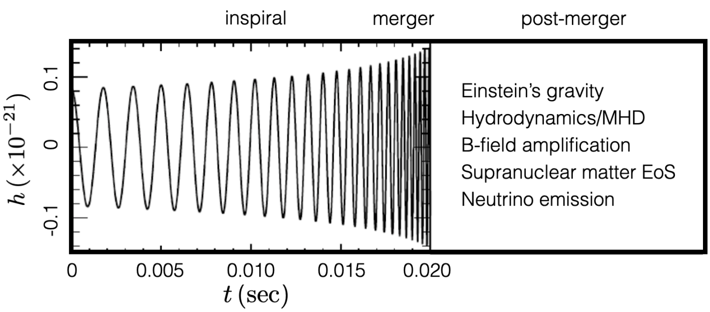

Fig. 1. Illustration of the coalescing part of the GW (chirp) signal of a BNS inspiral and merger. The form of the post-merger signal, not plotted, depends strongly on the physical ingredients incorporated in the numerical modelling.

Obtaining numerical relativity waveform models for BNS mergers is challenging: on the one hand, there are mathematical and physical difficulties associated with the presence of strong gravitational fields and magnetic fields, matter motion at relativistic speeds, shock waves, as well as aspects from nuclear physics which are not straightforward to simulate, as the transport of thermal and non-thermal radiation, the incorporation of nuclear reaction networks, or the access to tables of microphysical EoS. On the other hand, there are numerical difficulties associated with the absence of symmetries or issues inherent to Einstein's gravity such as the possible existence of coordinate degrees of freedom and curvature singularities, or the need to resolve simultaneously both the near zone (to model the source dynamics) and the wave zone (to compute the GW information). Finally, BNS merger simulations require significant computational resources in terms of both memory and power. This is aggravated by the large parameter space of the problem, limiting the ability to perform detailed parameter studies even when using supercomputers. Despite those many difficulties, numerical relativity simulations of BNS mergers have steadily progressed during the last 25 years, notably advancing the state-of-the-art in our knowledge of these systems (see reviews by [28, 33–36]).

The spacetime evolution equations are in most cases written down employing hyperbolic formulations such as BSSN [37, 38] or Z4 [39], and solved with high-order finite differencing or (pseudo-)spectral methods. On the other hand, the most widely adopted formulation of general relativistic hydrodynamics and MHD casts the hyperbolic systems of equations in flux-conservative form (in the so-called "Valencia" formulation [40, 41]) allowing for a solution procedure based on high-order, shock-capturing finite volume methods (employing either Riemann solvers of central schemes). Current simulations have reached a significant level of sophistication. Aspects worth highlighting involve the incorporation of individual spins in the initial data [42, 43], hence allowing for precessing orbits, and improvements on the treatment of the microphysics. In particular, the use of microphysical, finite-temperature EoS tables constructed using "tabulated" data from observations and nuclear physics experiments has now become routine (see *e.g.* [44–49]). This provides a self-consistent method for probing the impact of thermal effects on the fate of the binary remnant. Moreover, the amplification of magnetic fields by dynamical instabilities is also being incorporated in the modelling, either through direct numerical simulations with extreme resolutions [50, 51], or using sub-grid models to capture the growth of the instabilties at smaller scales [52–55]. Studying the effects of the magnetic field in the formation of collimated outflows and jets has also been possible [56–58]. Many groups are developing strategies to incorporate nuclear reaction networks into the simulation codes that allow to compute the nucleosynthetic yields and the kilonova emission in the late post-merger phase [59–63]. Likewise, simulations are starting to consider non-ideal fluids and dissipative effects [64–67]. Finally, implementing neutrino radiation transport is a major effort in current BNS merger simulations (see [68] for a recent review). All of these physical ingredients have an impact on the fate of the post-merger remnant and, as a result, on the associated GW emission. Their gradual incorporation in the numerical modelling will increase the faithfulness of the simulated post-merger waveforms which will certainly help future searches of those signals[1] in preparation for the significant increase in the amount of detections anticipated with third-generation observatories[2].

---

[1] A search for GWs from the remnant of the BNS merger GW170817 was reported in [69]. Both, short-duration (< 1 s) and intermediate-duration (< 500 s) signals, corresponding to GW emission from a hypermassive or supramassive neutron star, respectively, were considered. No signal from the post-merger remnant was found.

[2] In one year of operation, a network consisting of one Cosmic Explorer and the Einstein Telescope is expected to detect $\mathcal{O}(10^5)$ BNS mergers [70, 71].

2.2. PNS

Numerical simulations of CCSN have consistently shown that the main source of GW in the explosion of massive stars is not related to the violent hydrodynamical bounce that abruptly halts the gravitational collapse of the stellar core but it is rather associated with the subsequent excitation of the oscillation modes of the PNS during post-bounce evolution (see [72] and references therein). Therefore, at least potentially, the analysis of the eventual observations of GW signals from CCSN might help infer PNS properties. Such an accomplishment would make PNS asteroseismology possible, in the same way as helioseismology helps reveal the structure and dynamics of the Sun through the study of its oscillations.

The GW signals associated with PNS oscillations are highly stochastic. Most of the energy is stored in the so-called f-modes or g-modes (see below) whose frequencies depend on the mass and radius of the PNS, and are in general above 500 Hz. The waveforms may also contain low-frequency modes (below 500 Hz) triggered by the standing accretion shock instability (SASI). An example time-frequency (or spectrogram) plot of a post-bounce CCSN waveform is shown in Fig. 2. Distinct arch-shaped features are visible in the spectrogram, associated with characteristic vibration modes of the PNS. Such features are consistently observed in all numerical simulations of the post-bounce evolution of the PNS.

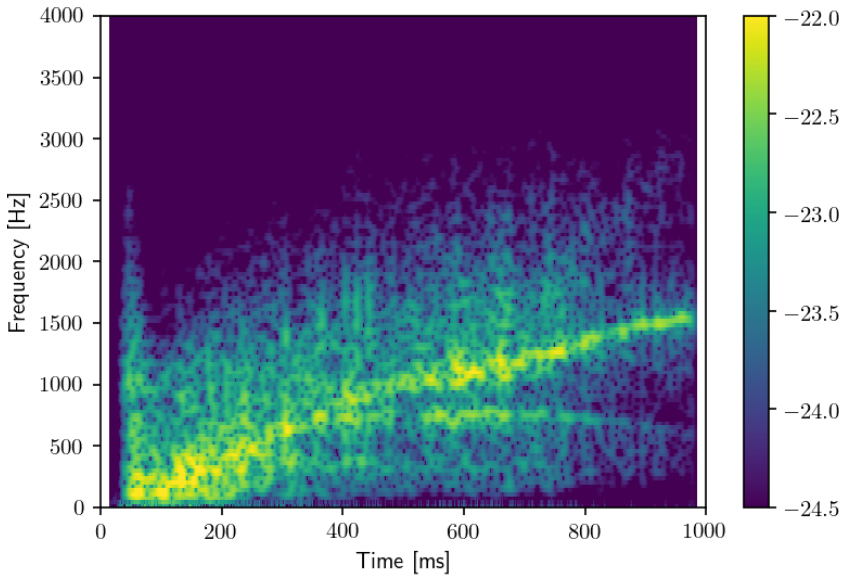

Fig. 2. Example of a PNS spectrogram. The arch-shaped features are associated with characteristic oscillation modes of the star. Colours indicate the power spectral density.

The most important quasi-normal modes of oscillation of neutron stars for GW emission are the f (fundamental), p (pressure), and g (gravity) polar fluid modes, the r (rotation) axial fluid modes (a subclass of inertial modes), and the w (wave) polar and axial spacetime modes. The f-mode exists only for non-radial oscillations and describes surface waves. This mode is due to the interface between the star and its surroundings and its eigenfunction has no nodes inside the star. The frequency of the f-mode is proportional to the square root of the average density of the star and has a typical value of $f \sim 2$ kHz, with a characteristic damping time $\tau < 1$ s. The p-modes exist for both radial and non-radial oscillations and there are infinitely many of them. Pressure is their restoring force and the oscillations are nearly radial. The frequencies of the p-modes depend on the travel time of acoustic waves across the star (standing sound waves), attaining typical values of $f > 4$ kHz with damping times $\tau > 1$ s. The g-modes only exist for finite temperature stars and there are infinitely many of them. Their restoring force is buoyancy and the oscillations are nearly tangential. The typical frequencies and damping times of the g-modes are $f < 500$ Hz and $\tau > 5$ s, respectively.

The idea of employing pulsating neutron stars for GW asteroseismology was put forward in the seminal work of [73]. By computing linear eigenfrequencies of the oscillation modes of neutron stars most important for GW astronomy (the f-mode, the first pressure p-mode, and the first w-mode) and using stellar models with twelve realistic EoS, a set of empirical relations between the mode-frequencies and the mass and radius of the star was inferred. The work of [73] was a proof-of-principle that those empirical relations can be used to extract properties of neutron stars from observed oscillation modes.

In the CCSN context, the characterization of the oscillation modes of the PNS can also be studied using linear perturbations of a spherical background, as an eigenvalue problem. Early attempts used simplified backgrounds based on Tolman–Oppenheimer–Volkoff (TOV) models [74–79]. More recent works employ a dynamical background from numerical simulations of CCSN [80–87]. In particular, Torres-Forné *et al.* [80, 82, 83] have developed the Great code (General Relativistic Eigenmode Analysis Tool)[3] which allows to compute PNS oscillation modes using a general-relativistic formalism that includes space-time perturbations on a dynamical background from simulations. This code is currently being upgraded to incorporate new solvers (spectral methods and Physics-Informed Neural Networks) and advection terms (accreting background, relevant for p-modes and SASI), while future extensions will account for rotating stars (adding rotation corrections to $g/f/p$-mode frequencies). Figure 3 shows that features

[3] www.uv.es/cerdupa/codes/GREAT

in the spectrograms can be matched to specific PNS eigenmodes. Shown are fits to two particular g-modes and to the f-mode, the fundamental pressure mode. Discerning which one is the dominant mode in a CCSN event and how the mode structure depends on the PNS properties might thus be possible after a successful detection of the gravitational waves produced in supernova explosions.

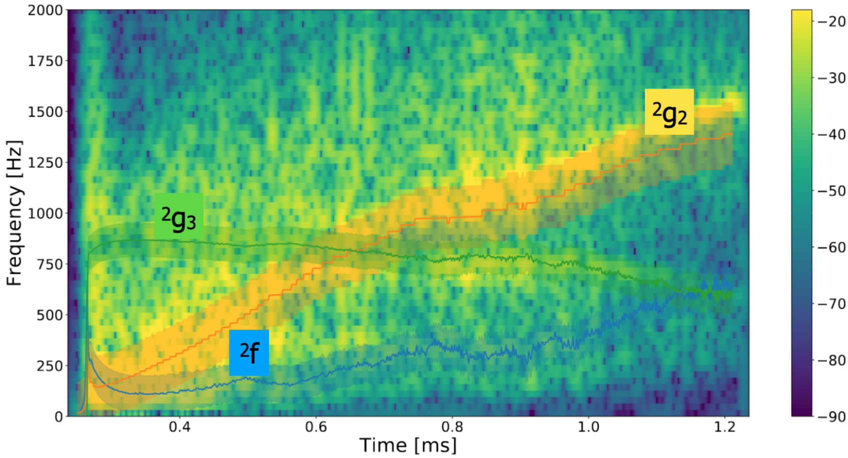

Fig. 3. Example of PNS eigenmodes. Shown are fits to two particular g-modes and to the f-mode.

3. Overview of recent results

3.1. BNS mergers

3.1.1. (Late) inspiral

Neutron stars in binary systems produce mutual tidal stresses that deform the metric around the stars in an EoS-dependent manner, through the tidal deformability parameter,

$$\Lambda = \frac{2}{3}\kappa_2 \left(\frac{R}{M}\right)^5 , \qquad (1)$$

where κ_2 is the quadrupolar Love number, R is the radius, and M is the mass of the star. Both R and κ_2 are fixed for a given stellar mass M by the EoS ($\kappa_2 = 0.05$–0.15 for realistic neutron stars). The tidal deformability parameter describes the degree at which a local metric suffers quadrupole deformations when in the tidal field of a companion. Large tidal effects on the late inspiral phase of a BNS merger have been observed in numerical simulations. The tidal deformability determines the $(l, m) = (2, 0)$ departure of the asymptotic metric from spherical symmetry and the departure of the waveform's orbital phase evolution from the point-particle form. The latter becomes significant as the GW frequency increases above ~ 600 Hz, *i.e.* only during the last few orbits before merger, and can be potentially observable.

In [88], Read *et al.* conducted a systematic investigation of the BNS inspiral using an extended set of EoS and a multiple-code effort to generate numerical-relativity waveforms. This study unveiled a quasi-universal (EoS-insensitive) relation between the peak GW frequency at merger and the tidal deformability. Quasi-universality implies that if the GW frequency at peak amplitude were observationally measured, the tidal deformability could be directly inferred from the empirical fit, and hence the moment of inertia and the compactness parameter M/R. Furthermore, the analytic relation between Λ and R given by Eq. (1) would yield the individual radii of the stars. Read *et al.* [88] concluded that with a single source at ~ 100 Mpc, the neutron star radius or Λ could be constrained to about 10%.

Signal GW170817 allowed to use the tidal deformability parameter to constrain the neutron star radius and EoS, as shown in [10]. The properties of the GW source were inferred by matching the data with predicted waveforms, conducting Bayesian analysis in the frequency range of 30–2048 Hz. The source-frame chirp mass was accurately constrained to be about $1.18\,M_\odot$. However, the estimates of the component masses are not as accurate as they are affected by the degeneracy between mass ratio and aligned spin components. Assuming a low-spin prior (consistent with the observed population), one obtains component masses $M_1 \in (1.36, 1.60)\,M_\odot$ and $M_2 \in (1.17, 1.36)\,M_\odot$. A single function $\Lambda(m)$ was computed from the static $l = 2$ perturbation of a TOV solution. The LVK Collaboration constraints on Λ_1 and Λ_2 disfavour (stiff) EoS that predict less compact stars, such as MS1 and MS1b, since the mass range recovered generates Λ values outside the 90% probability region. These results are consistent with radius constraints from X-ray observations of neutron stars.

3.1.2. Post-merger

Neutron stars aged $\sim 10^7$ years have undergone long-term cooling by neutrinos and photons. Hence, neutron stars in the late inspiral phase of a BNS merger are cold and can be modelled by zero-temperature EoS. As a result, the inspiral phase of a BNS coalescence event only probes cold EoS and thermal effects are not accessible. However, at merger and during the post-merger phase neutron stars heat up. Shock heating increases the temperature to about 10 MeV or more making finite-temperature effects likely to play an important dynamical role. Hence, neutron stars at those stages in the evolution of a BNS merger must be modelled by thermal EoS.

Loosely speaking, the fate of a BNS post-merger remnant can be twofold: it can be either a "hypermassive" neutron star (HMNS) where the remnant is supported by differential rotation and thermal gradients, or a "supramassive" neutron star, where the mass is small enough to be supported by rigid rotation. Numerical relativity simulations reveal that, fixing the EoS, a binary with a smaller mass will produce an HMNS which is further away from the stability threshold and will collapse to a black hole at a later time. Correspondingly, fixing the total mass, a binary with an EoS allowing for a larger thermal internal energy (*i.e.* hotter after merger) will have an increased pressure support and will collapse at a later time.

The post-merger phase has a rich GW phenomenology, with spectral features dominated by distinctive peaks that can be associated with specific oscillation modes of the remnant (see [89] and references therein for a recent study on this topic). The analysis of the spectra provides good prospects for constraining the thermal EoS of neutron stars. This is the ultimate goal of HMNS asteroseismology, specifically to use the GW spectra to find quasi-universal relations between oscillation frequencies (spectral peaks) and neutron star properties (*e.g.* mass, radius, tidal deformability). Indeed, numerical relativity simulations have revealed that a number of peculiar frequencies are related to the properties of the binary through quasi-universal relations. Those relations have been suggested for: (1) the GW frequency at merger [88–95], (2) the dominant peak frequency in the post-merger spectrum [88, 89, 92, 96–98], and (3) additional frequencies identifiable in the transient period right after merger [91, 92, 99]. While the early post-merger GW emission is dominated by the quadrupolar f-mode, the late post-merger emission is dominated by a low-frequency gravito-inertial mode triggered by convective instabilities in the remnant [100, 101]. Despite the fact that those modes have significantly less power than the f-mode, they might still be within reach of third-generation detectors, offering a possibility to infer rotational and thermal properties of BNS remnants [49, 102].

A robust method to characterize the GW emission from a BNS merger remnant is provided by Bayeswave [103, 104], a Bayesian GW data analysis pipeline developed within the LVK Collaboration[4]. This pipeline employs a morphology-independent approach to reconstruct the post-merger GW signal through a sum of basis functions (sine-Gaussians wavelets) and supply the full posterior probability distribution of the underlying waveform. Bayeswave has been applied on simulated data from numerical relativity simulations of BNS mergers injected into a network of advanced ground-based detectors [49, 102, 105–108].

[4] https://docs.ligo.org/lscsoft/bayeswave

The quality of the reconstruction is measured by the overlap between the signal s and the waveform model h

$$\mathcal{O} \equiv \frac{\langle s, h\rangle}{\sqrt{\langle s, s\rangle}\sqrt{\langle h, h\rangle}}\,, \tag{2}$$

where the inner product of two complex quantities is defined by

$$\langle a, b\rangle = 2\int_0^\infty \frac{a(f)b^*(f) + a^*(f)b(f)}{S_h(f)}\,\mathrm{d}f\,. \tag{3}$$

Here, the symbol * denotes complex conjugation and $S_h(f)$ is the one-sided noise power spectral density (PSD) of the detector. The GW signal reconstruction capabilities of Bayeswave allow one to obtain accurate posterior distributions for the GW peak frequency and for the neutron star radius, particularly as the SNR increases [107]. This property was used by [98] to obtain an estimate of the radius of a $1.6\,M_\odot$ non-rotating star, $R_{1.6}$, from a potential measurement of the peak frequency from the post-merger signal, as both quantities are correlated in an EoS-independent manner. The results show that the statistical error in the radius measurement from the post-merger signal is comparable to the corresponding error from the inspiral part of the waveform, yielding a measurement within 300–700 m at the 90% confidence level [98].

Numerical relativity simulations of BNS mergers also incorporate thermal effects in the post-merger phase where shock heating significantly increases the temperature. Early simulations adopted a hybrid approach to model the temperature dependence on the nuclear EoS [109], combining a collection of piecewise-polytropic EoS for the cold part and an ideal-gas-like EoS for the thermal part of the pressure, given by

$$p_{\mathrm{th}} = (\mathit{\Gamma}_{\mathrm{th}} - 1)(\varepsilon - \varepsilon_{\mathrm{cold}})\rho\,, \tag{4}$$

with $\mathit{\Gamma}_{\mathrm{th}} = 1.375$–$1.8$, and ε and ρ being the specific internal energy and density, respectively. Finite temperature adds further pressure support to the remnant that may change its internal structure and its subsequent evolution. Reference [110] showed that at densities above one-half of nuclear saturation density ($n_0 \approx 0.16$ fm^{-3}), $\mathit{\Gamma}_{\mathrm{th}}$ strongly depends on the nucleon effective mass. Hence, a hybrid approach may overestimate the thermal pressure by a few orders of magnitude [111] and may induce significant changes in the GW frequencies [112, 113]. To overcome this limitation, currently, most BNS simulations incorporate thermal effects through the full finite-temperature EoS.

Recently, the authors of [114] have compared pairs of BNS merger simulations in which the EoS is described by either a hybrid approach or a tabulated approach. This work focuses on whether the different treatment of thermal effects is imprinted in the GW spectra of the HMNS signal. The binaries consist of two identical irrotational neutron stars modelled by four hybrid EoS (SLy, APR4, H4, and MS1) composed of seven piecewise polytropic pieces and a thermal part with $\Gamma_{\rm th} = 1.8$. The corresponding tabulated models are built using the tables provided by [115] freely available at https://stellarcollapse.org/ The simulations show that a few ms after merger, heat production is much more significant in the tabulated EoS models, which exhibit a ring of higher temperature surrounding the HMNS. The most important dynamical difference was found for the LS220 EoS. In this case, the tabulated EoS model produces a stable HMNS, while in the simulation with the hybrid EoS treatment the remnant collapses promptly to a black hole.

Indeed, the different matter and spacetime dynamics are also imprinted on the gravitational waveforms. Figure 4 depicts the waveforms for the BNS simulations of [114] with the HShen EoS (left) and the DD2 EoS (right). The red curves correspond to the hybrid treatment of thermal effects, while the yellow curves correspond to the tabulated treatment. While no differences are found in the inspiral phase, the post-merger waveform is markedly different. In general, the oscillations of the HMNS are damped more rapidly for tabulated EoS model. Among all EoS considered by [114], the most significant differences in the post-merger waveform are found for the HShen EoS (see Fig. 4). The influence of these differences in the detectability prospects of BNS post-merger signals has been reported in [49, 116].

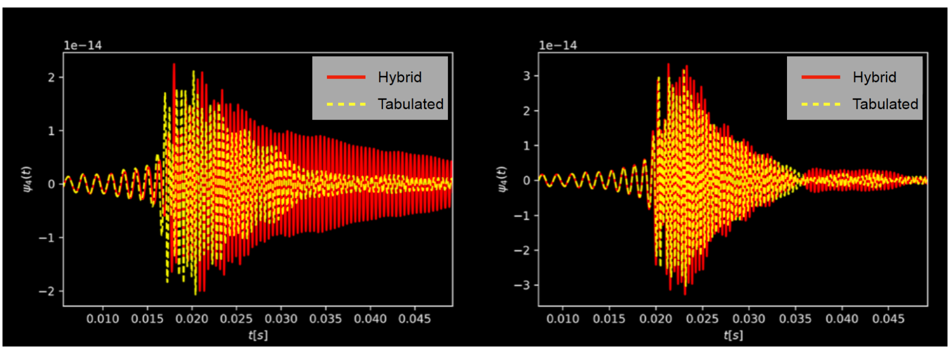

Fig. 4. Quadrupolar GW signals of two BNS mergers simulated by [114], HShen EoS (left) and DD2 EoS (right). Yellow and red waveforms refer to hybrid and tabulated models, respectively.

It is worth mentioning that non-convex dynamics, triggered by non-convex thermodynamics, might also play some role in BNS mergers. In classical fluid dynamics, the convexity of a system is determined by the EoS [117], more specifically, by the so-called fundamental derivative

$$\mathcal{G} \equiv -\frac{1}{2} V \, \frac{\left.\frac{\partial^2 p}{\partial V^2}\right|_s}{\left.\frac{\partial p}{\partial V}\right|_s} = 1 + \left.\frac{\partial \ln c_{\mathrm{s}}}{\partial \ln \rho_0}\right|_s . \tag{5}$$

In this equation, V denotes the specific volume, ρ_0 is the rest-mass density, c_{s} is the sound speed, and s is the specific entropy. The sign of the fundamental derivative measures the convexity of the isentropes in the pressure-density plane. If it is positive, isentropes are convex, leading to expansive rarefaction waves and compressive shocks. This is the usual regime in which many astrophysical scenarios develop. However, some EoS may display regimes in which the fundamental derivative is negative and the EoS is non-convex. Non-convexity yields exotic fluid dynamics, *e.g.* compressive rarefaction waves and expansive shocks. Fluids attaining negative values of the fundamental derivative are called Bethe–Zel'dovich–Thompson fluids [118–120] to highlight the pioneer work of these scientists in the study of EoS-driven, non-convex thermodynamics.

Non-convex dynamics may appear in neutron stars. At densities higher than nuclear saturation density n_0, nuclear/hadronic matter undergoes a phase transition into a quark–gluon plasma. In the crossover region the sound speed may become non-monotonic, a situation that can also result from the behaviour of the adiabatic index. The non-monotonicity of either quantity is a genuine feature of matter at a few times nuclear saturation density. Under such conditions, and particularly if there are phase transitions to exotic components of matter, the fundamental derivative could be negative, implying a non-convex EoS in that regime. This would lead to non-convex dynamics.

Recently, the authors of [121] illustrated the effects a non-convex EoS may produce on the dynamics of BNS mergers using a phenomenological EoS first employed by [122, 123] (a Gaussian "gamma-law" or GGL EoS). This toy-model EoS mimics the loss of convexity resulting from a non-monotonic behaviour of the adiabatic index with density. To do so, the pressure has the following functional form:

$$p = (\mathit{\Gamma} - 1)\rho\varepsilon \,, \qquad \mathit{\Gamma} = \gamma_0 + (\gamma_1 - \gamma_0) \exp\left[-\frac{(\rho - \rho_1)^2}{\sigma^2}\right] . \tag{6}$$

The results reported by [121] provide an explanation to the observable imprint of a first-order hadron–quark phase transition on the GW emission of

BNS mergers discussed in [124]. The latter found that the dominant post-merger GW frequency $f_{\rm peak}$ may exhibit a significant deviation from an empirical quasi-universal relation with the tidal deformability if a first-order phase transition leads to the formation of a stable extended quark-matter core in the post-merger remnant. The results reported by [121] indicate that the shift in frequency is ultimately associated with the appearance of anomalous dynamics triggered by the non-convexity of the EoS, and could also appear in EoS without phase transitions. Figure 5 shows that the empirical quasi-universal relation between the peak frequency and the tidal deformability is affected by non-convex dynamics, yielding, in some cases, to significant shifts in frequency. Those can be as large as 500 Hz for some choice of the parameters of the toy model GGL EoS (see [121] for specific details on the EoS parameters).

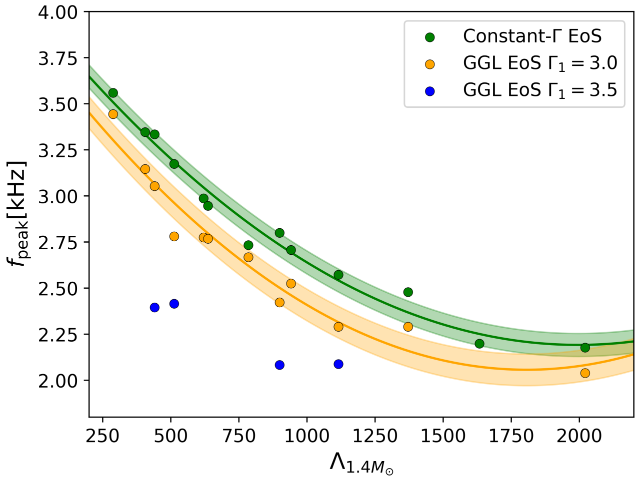

Fig. 5. GW peak frequency of the post-merger remnant $f_{\rm peak}$ as a function of the tidal deformability Λ. Each circle corresponds to one initial-data EoS, the corresponding colours indicating the EoS used in the evolutions (see the legend). Solid curves display the quasi-universal relations reported in [121]. Coloured regions represent the standard deviation of the corresponding fit.

3.2. PNS

Recent numerical work has addressed the feasibility of performing PNS asteroseismology with simulated waveforms from CCSN. In [83], empirical fits to the main PNS oscillation modes (the f-mode, p-modes, and g-modes) were built using 25 simulations of 8 CCSN progenitors (spanning a range of masses from $11.2M_\odot$ to $75M_\odot$), 6 EoS (LS220, Gshen-NL3, Hshen, SFHo, BHB-Λ, Hshen-Λ) and two different codes, Aenus-ALCAR [125, 126] and CoCoNuT [127]. It was found that the time-frequency relations (fits) of excited PNS modes are quasi-universal, as they do not depend on the EoS, progenitor star, or neutrino treatment. Those relations might potentially be used for parameter inference once actual GW observations from CCSN become available. The fits and quasi-universal relations reported in [83] have also been applied to independent 3D CCSN models studied by [19], obtaining remarkable agreement.

The use of those quasi-universal relations for detection and parameter inference has been reported in [128] and [129]. Both works focus on the $^2g_2$ mode, as this is the most salient feature in the spectrograms, with the goal of measuring the time evolution of the ratio $r = M_{\rm PNS}/R^2_{\rm PNS}$ (the surface gravity) in GW data. In the first step of the method, a model is built to relate this ratio to the frequency evolution of the GW signal, $r(f)$, using Aenus-ALCAR 1D simulations (model set) and the quasi-universal relations of [83]. In the second step, the method uses 2D simulations (test set) for which $r(t)$ is known to validate the model and provide detectability estimates.

In the study conducted by [128], waveforms are injected into 100 Gaussian noise realizations using the design Advanced LIGO PSD, assuming that the source is optimally oriented and the signal has been identified in the data. By varying the distance to the source, the reconstructed ratio is compared to the true ratio using as metrics the coverage (fraction of values within the 95% credible interval) and the relative error. It was found that the ratio is well reconstructed for most waveforms up to about 15 kpc (with a coverage greater than 80% and a relative error below 20%). Not surprisingly, the detectability prospects with third-generation detectors improve significantly, yielding a reconstructed ratio with good accuracy (median of coverage less than 95% of noise-only values) up to distances of 100–700 kpc. The study initiated in [128] was extended to a network of detectors in [129], including both the current second-generation network and the planned third-generation detectors. This is a more realistic working case as it takes into account the sky position of the source and the location/orientation of each ground-based detector. Since the location and orientation of the Einstein Telescope and of the Cosmic Explorer are not yet known, the Einstein Telescope detector was assumed for simplicity to be placed in the location of the Virgo detector with arbitrary orientation, while the two Cosmic Explorer sites were set according to [130], where a 40 km detector is located in Idaho and a smaller 20 km detector is in New Mexico. Furthermore, the network of five second-generation detectors (LHO, LLO, Virgo, KAGRA, and LAO) was considered at their nominal locations and design sensitivities. The results reported in [129] indicate that the current network of detectors at their design sensitivities is able to measure the ratio r of a Galactic CCSN for most of the progenitors considered, while a global network of the three third-generation detectors (CE20-CE40-ET) increases the distance reach to several hundred kpc from Earth.

Parameter inference studies of rapidly rotating CCSN progenitors have been reported in [131, 132]. Both works employ the waveform catalog produced in the comprehensive study of the CCSN bounce signal conducted by [133]. This catalog comprises over 1800 2D CCSN simulations (up to 10 ms post-bounce) that cover a parameter space of 98 different rotation profiles and 18 different EoS. The bounce GW signal is largely EoS-insensitive but instead is sensitive primarily to the ratio of rotational to gravitational energy, $T/|W|$, and at high-rotation rates, to the degree of differential rotation. The simulations of [133] show that the peak GW emission at bounce is related to the degree of oblateness of the core, which is related to the rotation rate. This study also reveals two main features in the bounce signal, a peak in the waveform with a well-defined amplitude Δh and several cycles of post-bounce oscillations with a distinctive frequency $f_{\rm peak}$, such that

$$\Delta h \propto \frac{T}{|W|}\,, \qquad f_{\rm peak} \propto \frac{1}{\sqrt{\rho_{\rm c}}}\,, \tag{7}$$

where ρ_c is the central rest-mass density of the PNS. A successful detection of the GW signal of a rotational CCSN might allow us to employ these functional dependences to estimate the source parameters $\rho_{\rm c}$ and $T/|W|$ by performing Bayesian inference on Δh and $f_{\rm peak}$.

Using the simulated waveforms of [133], Pastor-Marcos *et al.* [131] have recently assessed the feasibility of such parameter estimation. A key methodological aspect is the fact that a large fraction of the waveforms in the early post-bounce phase can be cast in a simple form — a master waveform template — depending only on $D\Delta h$ and $f_{\rm peak}$, where D is the distance to the source. This master template was used to perform a Bayesian analysis of waveforms injected in Gaussian-coloured noise for a network of three GW detectors formed by Advanced LIGO and Advanced Virgo. The results of [131] show that using the master waveform template for a Galactic event ($D \sim 10$ kpc), it is possible to recover the peak frequency and amplitude with an accuracy better than 10% for about 80% and 60% of the signals, respectively, assuming that the distance and inclination angle are known. As an example, Fig. 6 shows the median values and errors of the inferred posteriors depending on the injected values for the master template for quantities $f_{\rm peak}$, $D\,\Delta h\,\sin^2\theta$ (where θ is the inclination angle between the rotational axis of the core and the observer's line of sight), and ψ (polarization angle). Despite the fact that the results attained with the master template are promising, the study of [131] also shows that inference on waveforms that do not belong to the catalog of [133] (used to build the master template) is not sufficiently reliable.

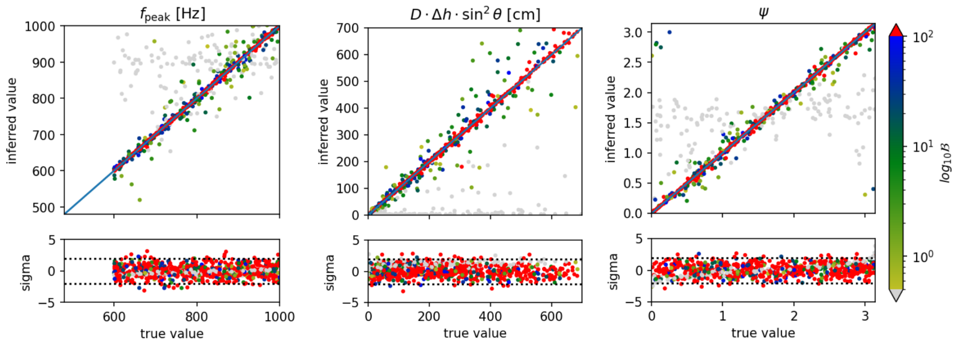

Fig. 6. Bayesian inference for the master template injections of [131]. Upper panels: Median of the inferred posteriors for $f_{\rm peak}$ (left panel), $D\,\Delta h\,\sin^2\theta$ (middle panel; θ is the inclination angle), and the waveform polarization angle ψ (right panel) as a function of the true value of the injected waveform. Colours indicate the logarithm of the Bayes factor. Values of $\log_{10}\mathcal{B} > 100$ are indicated in red and $\log_{10}\mathcal{B} < 0.5$ in grey. The blue solid line in the diagonal of all plots corresponds to equal true and inferred values. Lower panels: Error in the inferred values in terms of standard deviations. Horizontal dashed lines indicate the 2σ interval. See [131] for details.

We end by commenting on the recent work of Nunes *et al.* [132] who attempted to infer Δh and $f_{\rm peak}$ via a deep-learning approach (based on residual convolutional neural networks), instead of the Bayesian methodology employed in [131]. The same waveforms of [133] were injected into noise from the Advanced LIGO and Advanced Virgo detectors corresponding to the O2 and O3a observing runs. It was found that the inference of $f_{\rm peak}$ and Δh using neural networks can be successfully achieved, yielding results within the 1σ band from the expected (true) values (with the inference on $f_{\rm peak}$ systematically more accurate than that of Δh). The best model was also tested on waveforms from a recent CCSN catalog built by [134], different from the one used for the training of the neural network, finding that the true values of the two parameters for the new waveforms are mostly within the 1σ band around the network's predicted values. These results show that deep-learning techniques hold promise to infer physical parameters of Galactic rotational CCSN events.

4. Summary

The detection of gravitational waves by the LVK Collaboration detector network is having a major impact on our understanding of stellar-origin compact objects. Key properties of neutron stars such as their equation of state, mass, radius, or tidal deformability, can be inferred from the analysis of the gravitational waves they emit. This paper has reviewed the prospects to detect gravitational waves from two "types" of neutron stars — the hypermassive neutron star resulting from the merger of two neutron stars in a binary system, and the proto-neutron star born after the gravitational collapse of the core of a massive star. We have discussed the importance of performing numerical simulations of neutron stars in these astrophysical systems to understand their highly dynamical formation and to assist in the detection of the gravitational waves produced. Finally, we have considered a few selected investigations to illustrate ongoing efforts to infer neutron star parameters from the analysis of the gravitational-wave signals.

This work is supported by the Spanish Agencia Estatal de Investigación (PID2021-125485NB-C21) funded by MCIN/AEI/10.13039/501100011033 and ERDF A way of making Europe, by the Generalitat Valenciana (grant CIPROM/2022/49), and by the European Horizon Europe staff exchange (SE) programme HORIZON-MSCA-2021-SE-01 (NewFunFiCO-101086251).

REFERENCES

[1] B.P. Abbott *et al.*, «Observation of Gravitational Waves from a Binary Black Hole Merger», *Phys. Rev. Lett.* **116**, 061102 (2016).

[2] LIGO Collaboration (J. Aasi *et al.*), «Advanced LIGO», *Class. Quantum Grav.* **32**, 074001 (2015).

[3] F. Acernese *et al.*, «Advanced Virgo: a second-generation interferometric gravitational wave detector», *Class. Quantum Grav.* **32**, 024001 (2015).

[4] T. Akutsu *et al.*, «Overview of KAGRA: Detector design and construction history», *Prog. Theor. Exp. Phys.* **2021**, 05A101 (2021).

[5] R. Abbott *et al.*, «Open data from the first and second observing runs of Advanced LIGO and Advanced Virgo», *SoftwareX* **13**, 100658 (2021).

[6] R. Abbott *et al.*, «Open Data from the Third Observing Run of LIGO, Virgo, KAGRA, and GEO», *Astrophys. J. Suppl. Ser.* **267**, 29 (2023).

[7] LIGO, Virgo, and KAGRA collaborations (R. Abbott *et al.*) , «Population of Merging Compact Binaries Inferred Using Gravitational Waves through GWTC-3», *Phys. Rev. X* **13**, 011048 (2023).

[8] R. Abbott *et al.*, «Constraints on the Cosmic Expansion History from GWTC–3», *Astrophys. J.* **949**, 76 (2023).

[9] LIGO and Virgo collaborations (R. Abbott *et al.*), «Tests of general relativity with binary black holes from the second LIGO–Virgo gravitational-wave transient catalog», *Phys. Rev. D* **103**, 122002 (2021).

[10] LIGO and Virgo collaborations (B.P. Abbott *et al.*), «GW170817: Observation of Gravitational Waves from a Binary Neutron Star Inspiral», *Phys. Rev. Lett.* **119**, 161101 (2017).

[11] B.P. Abbott *et al.*, «Multi-messenger Observations of a Binary Neutron Star Merger», *Astrophys. J. Lett.* **848**, L12 (2017).

[12] B.P. Abbott *et al.*, «Gravitational Waves and Gamma-rays from a Binary Neutron Star Merger: GW170817 and GRB 170817A», *Astrophys. J. Lett.* **848**, L13 (2017).

[13] B.P. Abbott *et al.*, «Estimating the Contribution of Dynamical Ejecta in the Kilonova Associated with GW170817», *Astrophys. J. Lett.* **850**, L39 (2017).

[14] N. Christensen, «Stochastic gravitational wave backgrounds», *Rep. Prog. Phys.* **82**, 016903 (2019).

[15] B.P. Abbott *et al.*, «A guide to LIGO–Virgo detector noise and extraction of transient gravitational-wave signals», *Class. Quantum Grav.* **37**, 055002 (2020).

[16] W. Li *et al.*, «Nearby supernova rates from the Lick Observatory Supernova Search — II. The observed luminosity functions and fractions of supernovae in a complete sample», *Mon. Not. R. Astron. Soc.* **412**, 1441 (2011).

[17] R. Chapman, N.R. Tanvir, R.S. Priddey, A.J. Levan, «How common are long gamma-ray bursts in the local Universe?», *Mon. Not. R. Astron. Soc. Lett.* **382**, L21 (2007).

[18] S.E. Gossan *et al.*, «Observing gravitational waves from core-collapse supernovae in the advanced detector era», *Phys. Rev. D* **93**, 042002 (2016).

[19] J. Powell, B. Müller, «Gravitational wave emission from 3D explosion models of core-collapse supernovae with low and normal explosion energies», *Mon. Not. R. Astron. Soc.* **487**, 1178 (2019).

[20] S.M. Adams *et al.*, «Observing the Next Galactic Supernova», *Astrophys. J.* **778**, 164 (2013).

[21] M. Maggiore *et al.*, «Science case for the Einstein telescope», *J. Cosmol. Astropart. Phys.* **2020**, 050 (2020).

[22] M. Evans *et al.*, «A Horizon Study for Cosmic Explorer: Science, Observatories, and Community», `arXiv:2109.09882 [astro-ph.IM]`.

[23] M. Drago *et al.*, «*coherent WaveBurst*, a pipeline for unmodeled gravitational-wave data analysis», *SoftwareX* **14**, 100678 (2021).

[24] P.J. Sutton *et al.*, «X-Pipeline: an analysis package for autonomous gravitational-wave burst searches», *New J. Phys.* **12**, 053034 (2010).

[25] N.J. Cornish *et al.*, «BayesWave analysis pipeline in the era of gravitational wave observations», *Phys. Rev. D* **103**, 044006 (2021).

[26] (LIGO and Virgo collaborations (B.P. Abbott *et al.*), «First targeted search for gravitational-wave bursts from core-collapse supernovae in data of first-generation laser interferometer detectors», *Phys. Rev. D* **94**, 102001 (2016).

[27] M.J. Szczepańczyk *et al.*, «Optically targeted search for gravitational waves emitted by core-collapse supernovae during the third observing run of Advanced LIGO and Advanced Virgo», *Phys. Rev. D* **110**, 042007 (2024).

[28] K. Chatziioannou *et al.*, «Compact binary coalescences: gravitational-wave astronomy with ground-based detectors», `arXiv:2409.02037 [gr-qc]`.

[29] L. Blanchet, «Post-Newtonian theory for gravitational waves», *Living Rev. Relativ.* **27**, 4 (2024).

[30] A. Buonanno, T. Damour, «Effective one-body approach to general relativistic two-body dynamics», *Phys. Rev. D* **59**, 084006 (1999).

[31] A. Buonanno, T. Damour, «Transition from inspiral to plunge in binary black hole coalescences», *Phys. Rev. D* **62**, 064015 (2000).

[32] T. Damour, A. Nagar, «Comparing effective-one-body gravitational waveforms to accurate numerical data», *Phys. Rev. D* **77**, 024043 (2008).

[33] L. Baiotti, L. Rezzolla, «Binary neutron star mergers: a review of Einstein's richest laboratory», *Rep. Prog. Phys.* **80**, 096901 (2017).

[34] M.D. Duez, Y. Zlochower, «Numerical relativity of compact binaries in the 21st century», *Rep. Prog. Phys.* **82**, 016902 (2019).

[35] M. Shibata, K. Hotokezaka, «Merger and Mass Ejection of Neutron Star Binaries», *Annu. Rev. Nucl. Part. Sci.* **69**, 41 (2019).

[36] R. Ciolfi, «The key role of magnetic fields in binary neutron star mergers», *Gen. Relativ. Gravit.* **52**, 59 (2020).

[37] T.W. Baumgarte, S.L. Shapiro, «Numerical integration of Einstein's field equations», *Phys. Rev. D* **59**, 024007 (1998).

[38] M. Shibata, T. Nakamura, «Evolution of three-dimensional gravitational waves: Harmonic slicing case», *Phys. Rev. D* **52**, 5428 (1995).

[39] D. Alic *et al.*, «Conformal and covariant formulation of the Z4 system with constraint-violation damping», *Phys. Rev. D* **85**, 064040 (2012).

[40] F. Banyuls *et al.*, «Numerical $\{3+1\}$ General Relativistic Hydrodynamics: A Local Characteristic Approach», *Astrophys. J.* **476**, 221 (1997).

[41] L. Antón *et al.*, «Numerical 3+1 General Relativistic Magnetohydrodynamics: A Local Characteristic Approach», *Astrophys. J.* **637**, 296 (2006).

[42] W. Tichy *et al.*, «Constructing binary neutron star initial data with high spins, high compactnesses, and high mass ratios», *Phys. Rev. D* **100**, 124046 (2019).

[43] A. Rashti, A. Noe, «Realistic binary neutron star initial data with Elliptica», *Class. Quantum Grav.* **42**, 015007 (2025), `arXiv:2407.01701 [gr-qc]`.

[44] A. Bauswein, H.-T. Janka, R. Oechslin, «Testing Approximations of Thermal Effects in Neutron Star Merger Simulations», *Phys. Rev. D* **82**, 084043 (2010).

[45] Y. Sekiguchi, K. Kiuchi, K. Kyutoku, M. Shibata, «Gravitational Waves and Neutrino Emission from the Merger of Binary Neutron Stars», *Phys. Rev. Lett.* **107**, 051102 (2011).

[46] J. Fields *et al.*, «Thermal Effects in Binary Neutron Star Mergers», *Astrophys. J. Lett.* **952**, L36 (2023).

[47] P.L. Espino, G. Bozzola, V. Paschalidis, «Quantifying uncertainties in general relativistic magnetohydrodynamic codes», *Phys. Rev. D* **107**, 104059 (2023).

[48] L.R. Werneck *et al.*, «Addition of tabulated equation of state and neutrino leakage support to illinoisgrmhd», *Phys. Rev. D* **107**, 044037 (2023).

[49] M. Miravet-Tenés *et al.*, «Identifying thermal effects in neutron star merger remnants with model-agnostic waveform reconstructions and third-generation detectors», *Phys. Rev. D* **111**, 043006 (2025), `arXiv:2401.02493 [gr-qc]`.

[50] K. Kiuchi *et al.*, «Efficient magnetic-field amplification due to the Kelvin–Helmholtz instability in binary neutron star mergers», *Phys. Rev. D* **92**, 124034 (2015).

[51] K. Kiuchi, «General relativistic magnetohydrodynamics simulations for binary neutron star mergers», in: C. Bambi, Y. Mizuno, S. Shashank, F. Yuan (Eds.) «New Frontiers in GRMHD Simulations», Springer Series in Astrophysics and Cosmology, *Springer*, Singapore 2025, pp. 529–572, `arXiv:2405.10081 [astro-ph.HE]`.

[52] C. Palenzuela *et al.*, «Turbulent magnetic field amplification in binary neutron star mergers», *Phys. Rev. D* **106**, 023013 (2022).

[53] M. Miravet-Tenés, P. Cerdá-Durán, M. Obergaulinger, J.A. Font, «Assessment of a new sub-grid model for magnetohydrodynamical turbulence. I. Magnetorotational instability», *Mon. Not. R. Astron. Soc.* **517**, 3505 (2022).

[54] M. Miravet-Tenés, P. Cerdá-Durán, M. Obergaulinger, J.A. Font, «Assessment of a new sub-grid model for magnetohydrodynamical turbulence. II. Kelvin-Helmholtz instability», *Mon. Not. R. Astron. Soc.* **527**, 1081 (2023).

[55] D. Radice, I. Hawke, «Turbulence modelling in neutron star merger simulations», *Living Rev. Comput. Astrophys.* **10**, 1 (2024).

[56] M. Ruiz, A. Tsokaros, S.L. Shapiro, «Jet launching from merging magnetized binary neutron stars with realistic equations of state», *Phys. Rev. D* **104**, 124049 (2021).

[57] E.R. Most, E. Quataert, «Flares, Jets, and Quasiperiodic Outbursts from Neutron Star Merger Remnants», *Astrophys. J. Lett.* **947**, L15 (2023).

[58] K. Hayashi *et al.*, «Jet from binary neutron star merger with prompt black hole formation», `arXiv:2410.10958 [astro-ph.HE]`.

[59] A. Perego *et al.*, «Production of Very Light Elements and Strontium in the Early Ejecta of Neutron Star Mergers», *Astrophys. J.* **925**, 22 (2022).

[60] L. Jens Papenfort, E.R. Most, S. Tootle, L. Rezzolla, «Impact of extreme spins and mass ratios on the post-merger observables of high-mass binary neutron stars», *Mon. Not. R. Astron. Soc.* **513**, 3646 (2022).

[61] S. Fujibayashi *et al.*, «Comprehensive Study of Mass Ejection and Nucleosynthesis in Binary Neutron Star Mergers Leaving Short-lived Massive Neutron Stars», *Astrophys. J.* **942**, 39 (2023).

[62] L. Combi, D.M. Siegel, «Jets from Neutron-Star Merger Remnants and Massive Blue Kilonovae», *Phys. Rev. Lett.* **131**, 231402 (2023).

[63] A. Neuweiler *et al.*, «Long-term simulations of dynamical ejecta: Homologous expansion and kilonova properties», *Phys. Rev. D* **107**, 023016 (2023).

[64] M. Shibata, K. Kiuchi, «Gravitational waves from remnant massive neutron stars of binary neutron star merger: Viscous hydrodynamics effects», *Phys. Rev. D* **95**, 123003 (2017).

[65] E.R. Most *et al.*, «Projecting the likely importance of weak-interaction-driven bulk viscosity in neutron star mergers», *Mon. Not. R. Astron. Soc.* **509**, 1096 (2021).

[66] G. Camelio *et al.*, «Simulating bulk viscosity in neutron stars. I. Formalism», *Phys. Rev. D* **107**, 103031 (2023).

[67] P.L. Espino *et al.*, «Neutrino Trapping and Out-of-Equilibrium Effects in Binary Neutron-Star Merger Remnants», *Phys. Rev. Lett.* **132**, 211001 (2024).

[68] F. Foucart, «Neutrino transport in general relativistic neutron star merger simulations», *Living Rev. Comput. Astrophys.* **9**, 1 (2023).

[69] B.P. Abbott *et al.*, «Search for Post-merger Gravitational Waves from the Remnant of the Binary Neutron Star Merger GW170817», *Astrophys. J. Lett.* **851**, L16 (2017).

[70] M. Evanetal, «A Horizon Study for Cosmic Explorer: Science, Observatories, and Community», `arXiv:2109.09882 [astro-ph.IM]`.

[71] K. Walker, R. Smith, E. Thrane, D.J. Reardon, «Precision constraints on the neutron star equation of state with third-generation gravitational-wave observatories», *Phys. Rev. D* **110**, 043013 (2024).

[72] E. Abdikamalov, G. Pagliaroli, D. Radice, «Gravitational Waves from Core-Collapse Supernovae», in: C. Bambi, S. Katsanevas, K.D. Kokkotas (Eds.) «Handbook of Gravitational Wave Astronomy», *Springer Nature Singapore*, Singapore 2022, p. 21.

[73] N. Andersson, K.D. Kokkotas, «Towards gravitational wave asteroseismology», *Mon. Not. R. Astron. Soc.* **299**, 1059 (1998).

[74] A. Reisenegger, P. Goldreich, «A New Class of g-Modes in Neutron Stars», *Astrophys. J.* **395**, 240 (1992).

[75] V. Ferrari, G. Miniutti, J.A. Pons, «Gravitational waves from newly born, hot neutron stars», *Mon. Not. R. Astron. Soc.* **342**, 629 (2003).

[76] V. Ferrari, L. Gualtieri, J.A. Pons, A. Stavridis, «Rotational effects on the oscillation frequencies of newly born proto-neutron stars», *Mon. Not. R. Astron. Soc.* **350**, 763 (2004).

[77] A. Passamonti, M. Bruni, L. Gualtieri, C.F. Sopuerta, «Coupling of radial and nonradial oscillations of relativistic stars: Gauge-invariant formalism», *Phys. Rev. D* **71**, 024022 (2005).

[78] G. Camelio *et al.*, «Evolution of a proto-neutron star with a nuclear many-body equation of state: Neutrino luminosity and gravitational wave frequencies», *Phys. Rev. D* **96**, 043015 (2017).

[79] H. Sotani, T. Kuroda, T. Takiwaki, K. Kotake, «Probing mass-radius relation of protoneutron stars from gravitational-wave asteroseismology», *Phys. Rev. D* **96**, 063005 (2017).

[80] A. Torres-Forné, P. Cerdá-Durán, A. Passamonti, J.A. Font, «Towards asteroseismology of core-collapse supernovae with gravitational-wave observations — I. Cowling approximation», *Mon. Not. R. Astron. Soc.* **474**, 5272 (2018).

[81] V. Morozova, D. Radice, A. Burrows, D. Vartanyan, «The Gravitational Wave Signal from Core-collapse Supernovae», *Astrophys. J.* **861**, 10 (2018).

[82] A. Torres-Forné *et al.*, «Towards asteroseismology of core-collapse supernovae with gravitational wave observations — II. Inclusion of space-time perturbations», *Mon. Not. R. Astron. Soc.* **482**, 3967 (2019).

[83] A. Torres-Forné *et al.*, «Universal Relations for Gravitational-Wave Asteroseismology of Protoneutron Stars», *Phys. Rev. Lett.* **123**, 051102 (2019).

[84] D. Radice *et al.*, «Characterizing the Gravitational Wave Signal from Core-collap Supernovae», *Astrophys. J. Lett.* **876**, L9 (2019).

[85] H. Sotani, T. Kuroda, T. Takiwaki, K. Kotake, «Dependence of the outer boundary condition on protoneutron star asteroseismology with gravitational-wave signatures», *Phys. Rev. D* **99**, 123024 (2019).

[86] J.R. Westernacher-Schneider *et al.*, «Multimessenger asteroseismology of core-collapse supernovae», *Phys. Rev. D* **100**, 123009 (2019).

[87] N.E. Wolfe *et al.*, «Gravitational Wave Eigenfrequencies from Neutrino-driven Core-collapse Supernovae», *Astrophys. J.* **954**, 161 (2023).

[88] J.S. Read *et al.*, «Matter effects on binary neutron star waveforms», *Phys. Rev. D* **88**, 044042 (2013).

[89] K. Topolski, S.D. Tootle, L. Rezzolla, «Post-merger Gravitational-wave Signal from Neutron-star Binaries: A New Look at an Old Problem», *Astrophys. J.* **960**, 86 (2024).

[90] S. Bernuzzi *et al.*, «Quasiuniversal Properties of Neutron Star Mergers», *Phys. Rev. Lett.* **112**, 201101 (2014).

[91] K. Takami, L. Rezzolla, L. Baiotti, «Spectral properties of the post-merger gravitational-wave signal from binary neutron stars», *Phys. Rev. D* **91**, 064001 (2015).

[92] L. Rezzolla, K. Takami, «Gravitational-wave signal from binary neutron stars: A systematic analysis of the spectral properties», *Phys. Rev. D* **93**, 124051 (2016).

[93] E.R. Most *et al.*, «Signatures of Quark-Hadron Phase Transitions in General-Relativistic Neutron-Star Mergers», *Phys. Rev. Lett.* **122**, 061101 (2019).

[94] A. Bauswein *et al.*, «Identifying a First-Order Phase Transition in Neutron-Star Mergers through Gravitational Waves», *Phys. Rev. Lett.* **122**, 061102 (2019).

[95] L.R. Weih, M. Hanauske, L. Rezzolla, «Postmerger Gravitational-Wave Signatures of Phase Transitions in Binary Mergers», *Phys. Rev. Lett.* **124**, 171103 (2020).

[96] R. Oechslin, H.-T. Janka, «Gravitational Waves from Relativistic Neutron-Star Mergers with Microphysical Equations of State», *Phys. Rev. Lett.* **99**, 121102 (2007).

[97] N. Stergioulas, A. Bauswein, K. Zagkouris, H.-T. Janka, «Gravitational waves and non-axisymmetric oscillation modes in mergers of compact object binaries», *Mon. Not. R. Astron. Soc.* **418**, 427 (2011).

[98] A. Bauswein, H.-T. Janka, «Measuring Neutron-Star Properties via Gravitational Waves from Neutron-Star Mergers», *Phys. Rev. Lett.* **108**, 011101 (2012).

[99] A. Bauswein, N. Stergioulas, «Unified picture of the post-merger dynamics and gravitational wave emission in neutron star mergers», *Phys. Rev. D* **91**, 124056 (2015).

[100] R. De Pietri *et al.*, «Convective Excitation of Inertial Modes in Binary Neutron Star Mergers», *Phys. Rev. Lett.* **120**, 221101 (2018).

[101] R. De Pietri *et al.*, «Numerical-relativity simulations of long-lived remnants of binary neutron star mergers», *Phys. Rev. D* **101**, 064052 (2020).

[102] M. Miravet-Tenés *et al.*, «Prospects for the inference of inertial modes from hypermassive neutron stars with future gravitational-wave detectors», *Phys. Rev. D* **107**, 103053 (2023).

[103] N.J. Cornish, T.B. Littenberg, «BayesWave: Bayesian Inference for Gravitational Wave Bursts and Instrument Glitches», *Class. Quantum Grav.* **32**, 135012 (2015).

[104] N.J. Cornish *et al.*, «BayesWave analysis pipeline in the era of gravitational wave observations», *Phys. Rev. D* **103**, 044006 (2021).

[105] J. Clark *et al.*, «Prospects for high frequency burst searches following binary neutron star coalescence with advanced gravitational wave detectors», *Phys. Rev. D* **90**, 062004 (2014).

[106] J.A. Clark, A. Bauswein, N. Stergioulas, D. Shoemaker, «Observing gravitational waves from the post-merger phase of binary neutron star coalescence», *Class. Quantum Grav.* **33**, 085003 (2016).

[107] K. Chatziioannou *et al.*, «Inferring the post-merger gravitational wave emission from binary neutron star coalescences», *Phys. Rev. D* **96**, 124035 (2017).

[108] S. Bose *et al.*, «Neutron-Star Radius from a Population of Binary Neutron Star Mergers», *Phys. Rev. Lett.* **120**, 031102 (2018).

[109] J.S. Read, B.D. Lackey, B.J. Owen, J.L. Friedman, «Constraints on a phenomenologically parametrized neutron-star equation of state», *Phys. Rev. D* **79**, 124032 (2009).

[110] Y. Lim, J.W. Holt, «Enhanced adiabatic index for hot neutron-rich matter from microscopic nuclear forces», `arXiv:1909.09089 [nucl-th]`.

[111] C.A. Raithel, V. Paschalidis, F. Özel, «Realistic finite-temperature effects in neutron star merger simulations», *Phys. Rev. D* **104**, 063016 (2021).

[112] A. Bauswein, H.-T. Janka, R. Oechslin, «Testing approximations of thermal effects in neutron star merger simulations», *Phys. Rev. D* **82**, 084043 (2010).

[113] A. Figura *et al.*, «Binary neutron star merger simulations with hot microscopic equations of state», *Phys. Rev. D* **103**, 083012 (2021).

[114] D. Guerra *et al.*, «Thermal effects on long-lived remnants of binary neutron star mergers», in preparation, 2025.

[115] A.S. Schneider, L.F. Roberts, C.D. Ott, «Open-source nuclear equation of state framework based on the liquid-drop model with Skyrme interaction», *Phys. Rev. C* **96**, 065802 (2017).

[116] V. Villa-Ortega *et al.*, «Self-consistent treatment of thermal effects in neutron-star post-mergers: observational implications for third-generation gravitational-wave detectors», `arXiv:2310.20378 [gr-qc]`.

[117] R. Menikoff, B.J. Plohr, «The Riemann problem for fluid flow of real materials», *Rev. Mod. Phys.* **61**, 75 (1989).

[118] P.A. Thompson, «A Fundamental Derivative in Gasdynamics», *Phys. Fluids* **14**, 1843 (1971).

[119] Y.B. Zel'Dovich, «On the possibility of rarefaction shock waves», *Zh. Eksp. Teor. Fiz* **4**, 337 (1946).

[120] H.A. Bethe, «On the Theory of Shock Waves for an Arbitrary Equation of State», in: J.N. Johnson, R. Chéret (Eds.) «Classic Papers in Shock Compression Science», *Springer New York*, New York, NY 1998, pp. 421–495.

[121] G. Rivieccio, D. Guerra, M. Ruiz, J.A. Font, «Gravitational-wave imprints of nonconvex dynamics in binary neutron star mergers», *Phys. Rev. D* **109**, 064032 (2024).

[122] J.M. Ibáñez, A. Marquina, S. Serna, M.A. Aloy, «Anomalous dynamics triggered by a non-convex equation of state in relativistic flows», *Mon. Not. R. Astron. Soc.* **476**, 1100 (2018).

[123] M.A. Aloy *et al.*, «Neutron star collapse and gravitational waves with a non-convex equation of state», *Mon. Not. R. Astron. Soc.* **484**, 4980 (2019).

[124] A. Bauswein *et al.*, «Identifying a First-Order Phase Transition in Neutron Star Mergers through Gravitational Waves», *Phys. Rev. Lett.* **122**, 061102 (2019).

[125] M. Obergaulinger, «Astrophysical magnetohydrodynamics and radiative transfer: numerical methods and applications», Ph.D. Thesis, Max-Planck-Institute for Astrophysics, Garching, January 2008.

[126] O. Just, M. Obergaulinger, H.-T. Janka, «A new multidimensional, energy-dependent two-moment transport code for neutrino-hydrodynamics», *Mon. Not. R. Astron. Soc.* **453**, 3387 (2015).

[127] H. Dimmelmeier *et al.*, «Combining spectral and shock-capturing methods: A new numerical approach for 3D relativistic core collapse simulations», *Phys. Rev. D* **71**, 064023 (2005).

[128] M.-A. Bizouard *et al.*, «Inference of protoneutron star properties from gravitational-wave data in core-collapse supernovae», *Phys. Rev. D* **103**, 063006 (2021).

[129] T. Bruel *et al.*, «Inference of protoneutron star properties in core-collapse supernovae from a gravitational-wave detector network», *Phys. Rev. D* **107**, 083029 (2023).

[130] S. Borhanian, «GWBENCH: a novel Fisher information package for gravitational-wave benchmarking», *Class. Quantum Grav.* **38**, 175014 (2021).

[131] C. Pastor-Marcos, «Bayesian inference from gravitational waves in fast-rotating, core-collapse supernovae», *Phys. Rev. D* **109**, 063028 (2024).

[132] S. Nunes *et al.*, «Deep-learning classification and parameter inference of rotational core-collapse supernovae», *Phys. Rev. D* **110**, 064037 (2024).

[133] S. Richers *et al.*, «Equation of state effects on gravitational waves from rotating core collapse», *Phys. Rev. D* **95**, 063019 (2017).

[134] A. Mitra, B. Shukirgaliyev, Y.S. Abylkairov, E. Abdikamalov, «Exploring supernova gravitational waves with machine learning», *Mon. Not. R. Astron. Soc.* **520**, 2473 (2023).